



This article appeared in a journal published by Elsevier. The attached copy is furnished to the author for internal non-commercial research and education use, including for instruction at the authors institution and sharing with colleagues.

Other uses, including reproduction and distribution, or selling or licensing copies, or posting to personal, institutional or third party websites are prohibited.

In most cases authors are permitted to post their version of the article (e.g. in Word or Tex form) to their personal website or institutional repository. Authors requiring further information regarding Elsevier's archiving and manuscript policies are encouraged to visit:

<http://www.elsevier.com/copyright>



Contents lists available at ScienceDirect

Journal of Luminescence

journal homepage: www.elsevier.com/locate/jlumin

Multiplication of electronic excitations in nanophosphors $\text{Lu}_2\text{O}_3:\text{Eu}^{3+}$ and $\text{Lu}_2\text{O}_3:\text{Tb}^{3+}$

Vladimir N. Makhov^{a,b,*}, Cheslav Lushchik^a, Aleksandr Lushchik^a, Marco Kirm^a, Zhi-Fang Wang^c, Wei-Ping Zhang^c, Min Yin^c, Jing-Tai Zhao^d

^a Institute of Physics, University of Tartu, 142 Riia Str., 51014 Tartu, Estonia

^b Lebedev Physical Institute, 53 Leninskii Prospect, 119991 Moscow, Russia

^c University of Science and Technology of China, 230026 Hefei, PR China

^d Shanghai Institute of Ceramics, 1295 Dingxi Road, 200050 Shanghai, PR China

ARTICLE INFO

Available online 5 April 2009

Keywords:

Nanocrystals

Multiplication of electronic excitations

Surface losses

Lu_2O_3

ABSTRACT

Luminescence properties of $\text{Lu}_2\text{O}_3:\text{Eu}^{3+}$ and $\text{Lu}_2\text{O}_3:\text{Tb}^{3+}$ nanocrystalline powders with the particle size varying from 46 to 6 nm were studied under excitation by synchrotron radiation in the photon energy range (up to ~ 22.5 eV) covering the region where the processes of multiplication of electronic excitation occur. It was found that the excitation spectra of Tb^{3+} emission from all $\text{Lu}_2\text{O}_3:\text{Tb}^{3+}$ nanopowders have similar behavior, whereas the shape of the excitation spectra of Eu^{3+} emission from $\text{Lu}_2\text{O}_3:\text{Eu}^{3+}$ nanopowders strongly depends on the particle size. The difference in the behavior of $\text{Lu}_2\text{O}_3:\text{Eu}^{3+}$ and $\text{Lu}_2\text{O}_3:\text{Tb}^{3+}$ nanophosphor systems was explained by different mechanisms of the energy transfer from the host to Eu^{3+} or Tb^{3+} ions (either the hole or electron recombination mechanism, respectively), which are differently influenced by losses of electronic excitations near the particle surface.

© 2009 Elsevier B.V. All rights reserved.

1. Introduction

The processes of multiplication of electronic excitations (MEE) at exciting photon energies exceeding two band gaps are considered as a possible way for the development of high-efficiency phosphors with quantum yields higher than 1 (see [1,2] and references therein). For such well-known oxide hosts like Y_2O_3 or Lu_2O_3 with rather wide valence bands, the threshold of MEE is observed in the range $3\text{--}4E_g$ due to restrictions related to the momentum (wave vector \mathbf{k}) conservation law. However, in nanocrystals (NCs) the requirement for momentum conservation is relaxed [3,4] and, generally, one can expect the lowering of the threshold of MEE, which would be particularly beneficial for rare-gas discharge-based lighting applications. On the other hand, the small size of particles in NCs can strongly limit the free mean path of mobile excitations, thus decreasing the probability of carrier's inelastic scattering responsible for the creation of secondary excitations.

Lu_2O_3 is a rather attractive host for rare-earth ($\text{Eu}^{3+}, \text{Tb}^{3+}$) doped X-ray phosphors [5] because of high stopping power for X-ray radiation due to high density (9.42 g/cm^3) and high Z-number of Lu (71). Lu_2O_3 is a structural analog of Y_2O_3 , which is the well-known host for Eu^{3+} - and Tb^{3+} -doped commercial

phosphors. The lattice structure of Lu_2O_3 provides two sites with different symmetry for doping rare-earth ions, namely the centrosymmetric C_{3i} (S_6) and low-symmetry C_2 sites. For the C_{3i} sites the electric dipole $4f\text{--}4f$ transitions are forbidden and emission spectra are dominated by transitions in the ions occupying the C_2 sites [6].

In the present work, the luminescence properties of $\text{Lu}_2\text{O}_3:\text{Eu}^{3+}$ and $\text{Lu}_2\text{O}_3:\text{Tb}^{3+}$ NC powders were investigated under excitation by synchrotron radiation with photon energies up to ~ 22.5 eV (i.e. up to $\sim 4E_g$), in order to reveal the features and mechanisms of MEE in nanophosphors.

2. Experiment

The experiments were carried out at the SUPERLUMI station of HASYLAB at DESY, using for excitation 3.75–22.5 eV synchrotron radiation from the DORIS storage ring [7]. The excitation spectra were measured with an instrumental resolution of ~ 0.3 nm. Emission spectra were recorded by using a 0.3 m Czerny–Turner monochromator-spectrograph SpectraPro-308i (Acton Research Inc.) with a photomultiplier tube (R6358P, Hamamatsu). The spectral resolution was ~ 1 nm. All measurements were performed at room temperature.

Nanoscale $\text{Lu}_2\text{O}_3:\text{Eu}^{3+}$ (5%) and $\text{Lu}_2\text{O}_3:\text{Tb}^{3+}$ (1%) powders with the particle size varied from 46 to 6 nm were prepared by solution combustion synthesis [8]. Nanopowders were slightly pressed into small copper cups (with a diameter of 3 mm and thickness of

* Corresponding author at: Institute of Physics, University of Tartu, Riia 142, 51014 Tartu, Estonia. Fax: +372 738 3033.

E-mail address: makhov@fi.tartu.ee (V.N. Makhov).

1 mm), which were then glued onto a sample holder in an UHV chamber.

3. Results and discussion

Although the emission intensity of both phosphor systems is reduced with the decrease of a particle size, as expected, the emission spectrum remains unchanged, showing only some broadening of the lines for the samples with the smallest particles (Figs. 1 and 2). The red emission of $\text{Lu}_2\text{O}_3:\text{Eu}^{3+}$ is due to the $^5\text{D}_0 \rightarrow ^7\text{F}_j$ transitions in Eu^{3+} . Green emission of $\text{Lu}_2\text{O}_3:\text{Tb}^{3+}$ arises from the $^5\text{D}_4 \rightarrow ^7\text{F}_j$ transitions in Tb^{3+} . Excitation spectra of Tb^{3+} green emission from all the studied $\text{Lu}_2\text{O}_3:\text{Tb}^{3+}$ NC samples (Fig. 3) have similar behavior in the whole spectral range showing the same features of intracenter excitation of Tb^{3+} at ~ 4.8 eV (due to spin-allowed $4f \rightarrow 5d$ transitions) and analogous onset of luminescence intensity increase near 14 eV. The latter corresponds to the threshold of MEE, as it was observed earlier for the “bulk” phosphor $\text{Y}_2\text{O}_3:\text{Tb}^{3+}$, in which the crystallites had

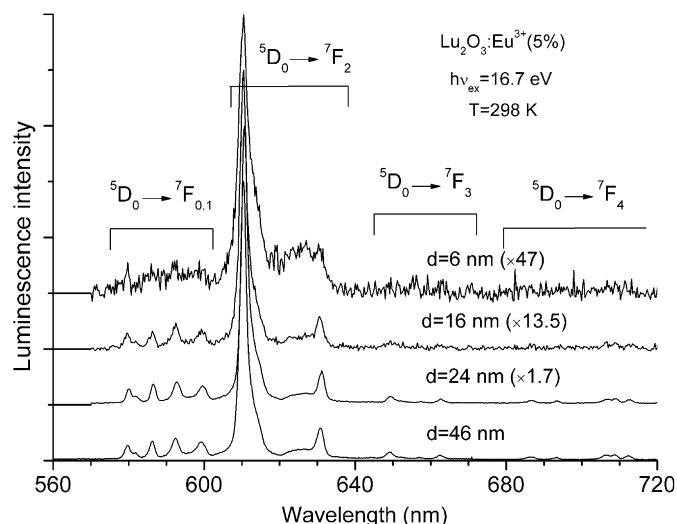


Fig. 1. Normalized emission spectra of $\text{Lu}_2\text{O}_3:\text{Eu}^{3+}$ nanopowders under excitation by 16.7 eV photons at room temperature. The assignments of emission lines to the corresponding $\text{Eu}^{3+} 4f^6 \rightarrow 4f^6$ transitions are given.

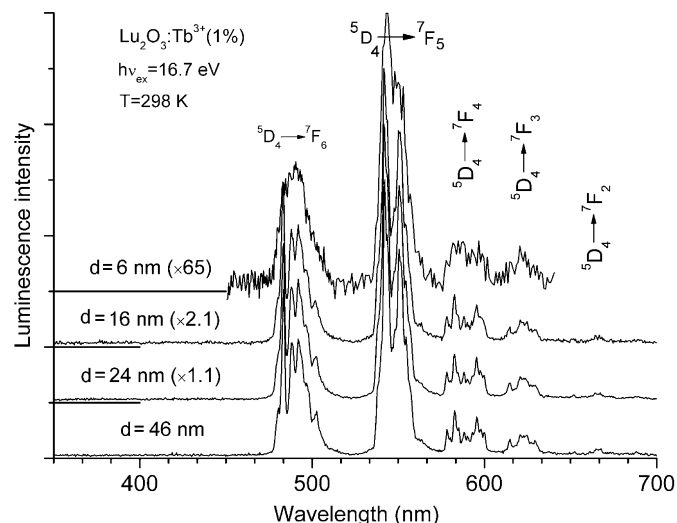


Fig. 2. Normalized emission spectra of $\text{Lu}_2\text{O}_3:\text{Tb}^{3+}$ nanopowders under excitation by 16.7 eV photons at room temperature. The assignments of emission lines to the corresponding $\text{Tb}^{3+} 4f^8 \rightarrow 4f^8$ transitions are given.

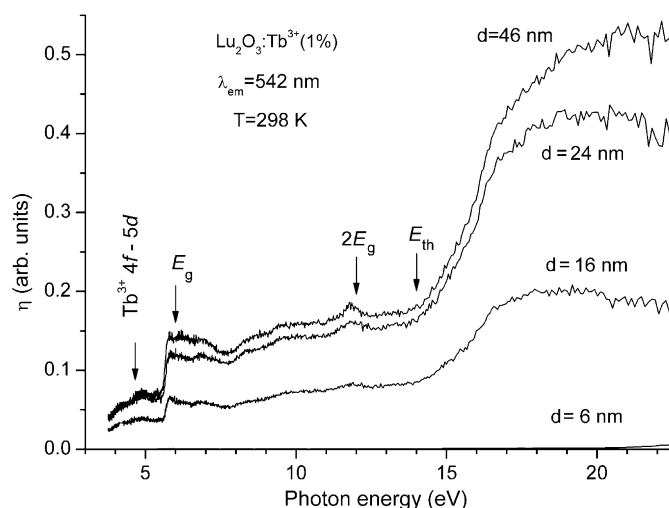


Fig. 3. Excitation spectra of $\text{Lu}_2\text{O}_3:\text{Tb}^{3+}$ nanopowders measured at room temperature monitoring $\text{Tb}^{3+} 5\text{D}_4 \rightarrow 7\text{F}_5$ emission at 542 nm. The energy of $\text{Tb}^{3+} 4f \rightarrow 5d$ transitions, the band-gap energy E_g and the MEE threshold energy E_{th} are marked.

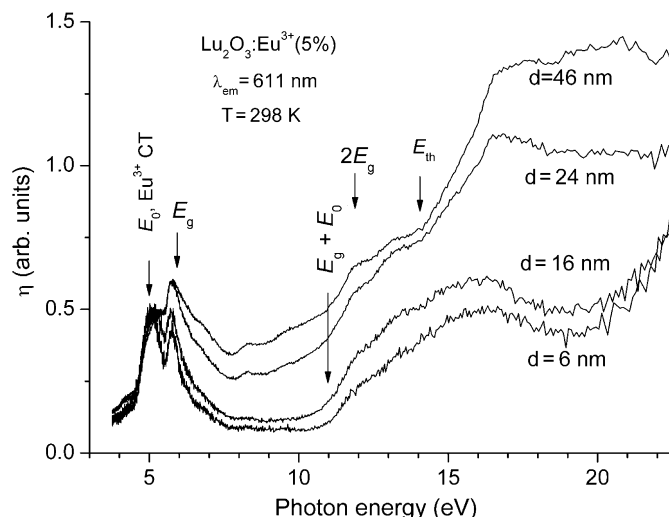


Fig. 4. Excitation spectra of $\text{Lu}_2\text{O}_3:\text{Eu}^{3+}$ nanopowders measured at room temperature monitoring $\text{Eu}^{3+} 5\text{D}_0 \rightarrow 7\text{F}_2$ emission at 611 nm. The spectra are normalized to the intensity of first CT band in the 5.05–5.4 eV region. The energy of Eu^{3+} charge-transfer transitions E_0 , the band-gap energy E_g , the threshold energy for impact excitation of $\text{Eu}^{3+} E_g + E_0$ and the MEE threshold energy E_{th} are marked.

typical grain size of several microns [9]. However, the shape of the excitation spectrum of Eu^{3+} red emission from the $\text{Lu}_2\text{O}_3:\text{Eu}^{3+}$ NC samples (Fig. 4) strongly depends on the particle size. The low-energy band of Eu^{3+} excitation, which is due to charge transfer (CT) $\text{O}^{2-} \rightarrow \text{Eu}^{3+}$ transitions, shows a notable red shift from ~ 5.4 to ~ 5.05 eV with the decreasing particle size from 46 to 6 nm particles, respectively. It agrees well with the results reported earlier in Ref. [8]. Furthermore, for the phosphors with smaller particle size the luminescence intensity in the region of band-to-band transitions at $h\nu > 6$ eV decreases relatively to that excited in the CT band. It has a rather small intensity for 6 nm particles in the region $h\nu = 7\text{--}11$ eV. However, in addition to the threshold at ~ 14 eV typical for the samples with large-sized particles or “bulk” phosphors $\text{Y}_2\text{O}_3:\text{Eu}^{3+}$ [9], another onset at lower photon energies ~ 11 eV appears in the spectrum.

The processes of MEE can be considered within a simplified model of a system with two parabolic energy bands, the extremes

of which are located in the center of the Brillouin zone, i.e. at $\mathbf{k} = 0$ [1,2]. If photoelectron created after the photon absorption has high enough kinetic energy, it can ionize the crystal as a result of inelastic scattering on valence electrons. The process of such impact ionization by hot photoelectrons takes place according to the energy conservation law and of crystal momentum (wave vector \mathbf{k}) conservation law. The direct interband transition with a photon absorption causes the creation of a hot conduction electron with effective mass m_e and a hot hole in a valence band with effective mass m_h . The excess of energy $h\nu - E_g$ is divided between a photoelectron and a photohole in accordance with the ratio m_h/m_e . If $m_e/m_h < 1$, a hot photoelectron gains a larger part of the photon energy. This primary electron is able to create a secondary $e-h$ pair if its energy E_i exceeds the value of E_g . The value of E_i should be actually larger than E_g in order to conserve the total wave vector for the inelastic scattering with the formation of a secondary $e-h$ pair. The threshold photon energy for secondary $e-h$ pair creation E_{th} equals $2E_g$ if $m_e \ll m_h$. The maximum value $E_{th} = 4E_g$ ($3E_g$ if the interaction of a hot photoelectron/photohole with phonons is taken into account) corresponds to the case $m_e/m_h = 1$, when a hot photoelectron and a hot photohole both have sufficient energies to create a secondary $e-h$ pair. Anyway, using this simple approach $E_{th} > 2E_g$ in all crystals, because a part of the absorbed energy is transferred to a photohole.

When applying more advanced theoretical approach: a multiple-parabolic-branch band model, which takes into account scattering processes in different branches of Brillouin zone beyond the above-mentioned single-parabolic-branch model, considerably lower thresholds for creation of secondary electronic excitations can be obtained in wide gap insulators [10]. The resulting theoretical values agree well with the experimental ones for the secondary exciton production in solid Xe [11] and similar processes have been discussed for other rare-gas solids [12]. However, in the case of NCs one has to keep in mind spatial limitations making situation different from bulk crystals. Therefore, in the first approximation we can avoid such effects when interpreting NCs results.

It is well known that for semiconductor NCs, the quantum confinement leads to the blue shift of the band-gap (as well as excitonic absorption) energy. However, in NCs of insulators the quantum confinement effects are not so pronounced even for very small particle sizes because of relatively small spatial extent of excitations in comparison with semiconductors (see, e.g., the review paper [13]). In particular, a weak quantum confinement effect in $Y_2O_3:Ce^{3+}$ and $Gd_2O_3:Eu^{3+}$ nanophosphors was revealed in Refs. [14,15]. On the other hand, in Ref. [16] it was shown that quantum confinement does not occur in Lu_2O_3 nanopowders for particle sizes down to at least 6 nm. This circumstance points to the fact that the momentum conservation law for such sizes of particles is still valid in Lu_2O_3 . Therefore, the momentum conservation law in MEE processes for all NC samples studied here should be always taken into account explicitly and the effects observed in the spectra are not resulting from the quantum confinement. This explains why in $Lu_2O_3:Tb^{3+}$ nanophosphors the threshold energy for MEE processes (at ~ 14 eV) is independent of the particle size. Also the features of excitation spectra for $Lu_2O_3:Eu^{3+}$ nanopowders are not assigned to quantum confinement phenomenon, but can be related to some surface effects prevailing in small particles.

It is assumed that the difference in the behavior of $Lu_2O_3:Eu^{3+}$ and $Lu_2O_3:Tb^{3+}$ phosphor systems is caused by various mechanisms of the energy transfer from the host to Eu^{3+} or Tb^{3+} ions (either hole or electron recombination mechanism, respectively), which are differently influenced by losses of electronic excitations near the particle surface. The hole recombination mechanism

suggests that the Eu^{3+} ion captures first the free electron: $Eu^{3+} + e^- \rightarrow Eu^{2+}$ and thereafter the hole recombines on the Eu^{2+} ion resulting in an ion in the excited state $(Eu^{3+})^*$, from which the characteristic luminescence of Eu^{3+} takes place. In the electron recombination mechanism the hole is captured first $Tb^{3+} + h^+ \rightarrow Tb^{4+}$, followed by recombination of the electron with the ion. As it has been already found earlier for the “bulk” phosphors based on the Y_2O_3 host [9] the surface losses strongly affect the efficiency of Eu^{3+} luminescence, whereas the influence of surface losses on luminescence of Tb^{3+} is very weak. The latter effect was explained by the more efficient capture of the slow holes by Tb^{3+} ions.

The decreasing of the size of particles obviously leads to larger influence of surface effects on nanophosphor luminescence. Accordingly, one can expect that for the $Lu_2O_3:Eu^{3+}$ nanophosphor the excitation spectra will be strongly modified with the changing of the particle size, whereas for the $Lu_2O_3:Tb^{3+}$ nanophosphor this effect should be less pronounced. This is just what we have observed in the experimental excitation spectra recorded by us. The shape of spectrum for the $Lu_2O_3:Tb^{3+}$ phosphors is practically the same for all particle sizes including the spectral range 6–14 eV, where the quantum efficiency forms a plateau in spite of the fact that absorption coefficient of Lu_2O_3 changes its value by about 10 times in this range (if we assume similar behavior of absorption as for Y_2O_3 [9]). The threshold energy of MEE at ~ 14 eV exceeds $2E_g$ but is less than $3E_g$, i.e. it can be well described within the above-mentioned simple model of MEE.

In the excitation spectra of the $Lu_2O_3:Eu^{3+}$ phosphors the quantum efficiency strongly decreases in the energy range 6–8 eV, where maximal increase of an absorption coefficient of the host is observed. This effect is presumably due to surface losses. As one can expect, the effect is more pronounced for smaller particles. In the range 8–11 eV, the quantum efficiency is extremely low for the smallest sizes of particles. In this range of exciting photon energy the free path of photoelectrons, before their capture by the Eu^{3+} ions, may exceed the size of the particles that will lead to almost complete absence of Eu^{3+} luminescence. However, when the kinetic energy of the hot photoelectron is high enough for the so-called impact excitation of an impurity ion [17] (which is more noticeable for elevated concentration of doping ions): $h\nu > E_g + E_0$ (E_0 is the energy of intracenter excitation of impurity ion), the free path of photoelectrons in such process can be shorter than that of their capturing (after thermalization) at the Eu^{3+} ions. Accordingly, the excitation spectrum will show the increase of luminescence intensity at photon energies above this threshold. According to simple MEE model, the threshold at 11 eV cannot be due to the creation of secondary $e-h$ pairs since this energy is smaller than $2E_g$.

4. Conclusions

The different behavior of excitation spectra of $Lu_2O_3:Eu^{3+}$ and $Lu_2O_3:Tb^{3+}$ nanophosphors has been revealed in the region of the host absorption, in particular in the energy range of MEE (i.e. at $h\nu = 2E_g - 4E_g$). The effect was interpreted as being due to different mechanisms of the energy transfer from the host to Eu^{3+} or Tb^{3+} ions (either hole or electron recombination mechanism, respectively), which are differently influenced by the losses of electronic excitations near the particle surface. The appearance of the onset at 11 eV in the excitation spectra of $Lu_2O_3:Eu^{3+}$ nanophosphors has been assigned to the impact excitation of Eu^{3+} ions by fast photoelectrons. The possible changes in the momentum conservation law do not significantly influence the mechanisms of MEE in $Lu_2O_3:Eu^{3+}$ and $Lu_2O_3:Tb^{3+}$ nanophosphors for the studied sizes of particles (down to 6 nm). However, in semiconductor nanomaterials with similar particle sizes, but with considerably larger spatial extent of excitations, the effect can be strong enough

for the enhancement of quantum yield of photoluminescence under excitation by photons with the energy near $2E_g$, i.e. well below the threshold of MEE for the bulk phosphors [4].

Acknowledgments

This work was supported by RFBR Grant 06-02-39027-NNSF, Estonian Science Foundation (Grant 6652), the European Community Research Infrastructure Action within the FP6 Program through the Contract RII3-CT-2004-506008 (IA-SFS), NSFC (No. 10774140), Funds for International Cooperation and Exchange of the NSFC (No. 50711120504), Specialized Research Fund for the Doctoral Program of Higher Education (No. 20060358054) and Special Foundation for Talents of Anhui Province, China (No. 2007Z021).

References

- [1] Ch.B. Lushchik, T.I. Savikhina, Bull. Acad. Sci. USSR Phys. Ser. 45 (1981) 34.
- [2] A. Lushchik, E. Feldbach, R. Kink, Ch. Lushchik, M. Kirm, I. Martinson, Phys. Rev. B 53 (1996) 5379.
- [3] M.S. Hybertsen, Phys. Rev. Lett. 72 (1994) 1514.
- [4] M.C. Beard, K.P. Knutsen, P. Yu, J.M. Luther, Q. Song, W. Metzger, R.J. Ellingson, A.J. Nozik, Nano Lett. 7 (2007) 2506.
- [5] A. Lempicki, C. Brecher, P. Szupryczynski, H. Lingertat, V.V. Nagarkar, S.V. Tipnis, S.R. Miller, Nucl. Instrum. Methods A 488 (2002) 579.
- [6] E. Zych, J. Phys.: Condens. Matter 14 (2002) 5637.
- [7] G. Zimmerer, Radiat. Meas. 42 (2007) 859.
- [8] M. Xu, W. Zhang, N. Dong, Y. Jiang, Y. Tao, M. Yin, J. Solid State Chem. 178 (2005) 477.
- [9] Yu.M. Aleksandrov, A.I. Kuznetsov, Ch.B. Lushchik, V.N. Makhov, I.A. Meriloo, T.I. Savikhina, T.I. Syreishchikova, M.N. Yakimenko, Tr. Inst. Fiz. Akad. Nauk Est. SSR 53 (1982) 7.
- [10] A.N. Vasil'ev, Y. Fang, V.V. Mikhailin, Phys. Rev. B 60 (1999) 5340.
- [11] B. Steeg, M. Kirm, V. Kisand, S. Kording, S. Vielhauer, G. Zimmerer, J. Low Temp. Phys. 111 (1998) 739.
- [12] M. Kirm, S. Vielhauer, G. Zimmerer, V. Kisand, E. Sombrowski, B. Steeg, Fiz. Nizk. Temp. 29 (2003) 1081.
- [13] P. Tanner, J. Nanosci. Nanotechnol. 5 (2005) 1455.
- [14] B. Mercier, C. Dujardin, G. Ledoux, D. Nicolas, B. Masenelli, P. Melinon, J. Lumin. 122–123 (2007) 756.
- [15] B. Mercier, G. Ledoux, C. Dujardin, D. Nicolas, B. Masenelli, P. Melinon, G. Bergeret, J. Chem. Phys. 126 (2007) 044507.
- [16] E. Zych, M. Wójtowicz, L. Kępiński, M.A. Małecka, Opt. Mater. 31 (2009) 241.
- [17] E. Feldbach, M. Kamada, M. Kirm, A. Lushchik, Ch. Lushchik, I. Martinson, Phys. Rev. B 56 (1997) 13,908.